

## Unifying length-scale-based rheology of dense suspensions

Zhuan Ge<sup>1,2</sup>, Teng Man<sup>2,\*</sup>, Herbert E. Huppert,<sup>3</sup>  
Kimberly M. Hill,<sup>4,†</sup> and Sergio Andres Galindo-Torres<sup>2,‡</sup>

<sup>1</sup>College of Civil Engineering and Architecture, Zhejiang University, 866 Yuhangtang Road, Hangzhou 310058, Zhejiang, China

<sup>2</sup>Key Laboratory of Coastal Environment and Resources of Zhejiang Province (KLaCER), School of Engineering, Westlake University, 18 Shilongshan Street, Hangzhou, Zhejiang 310024, China

<sup>3</sup>Institute of Theoretical Geophysics, King's College, University of Cambridge, King's Parade, Cambridge CB2 1ST, United Kingdom

<sup>4</sup>Department of Civil, Environmental, and Geo-Engineering, University of Minnesota, Minneapolis, Minnesota, USA



(Received 23 December 2022; accepted 28 November 2023; published 30 January 2024)

We present a length-scale-based rheology for dense sheared particle suspensions as they transition from inertial- to viscous-dominated. We derive a length-scale ratio using straightforward physics-based considerations for a particle subjected to pressure and drag forces. In doing so, we demonstrate that an appropriately chosen length-scale ratio intrinsically provides a consistent relationship between normal stress and system proximity to its “jammed” or solidlike state, even as a system transitions between inertial and viscous states, captured by a variable Stokes number.

DOI: [10.1103/PhysRevFluids.9.L012302](https://doi.org/10.1103/PhysRevFluids.9.L012302)

### I. INTRODUCTION

Particle flows and particle-fluid flows are ubiquitous in natural phenomena and industrial processes, such as landslides, debris flows, rock falls, and concrete [1–3]. Complex environmental conditions make it difficult to obtain a unified constitutive law for their flow characteristics, particularly for dense flows, where short-range interactions are enduring and often generate long-range correlations [4].

In last two decades, significant progress has been made in modeling wet and dry granular flows, focusing on dimensional analysis and time scales. For dry granular flows, the local normal stress  $P_p$  (which is associated with interparticle interactions only), particle density  $\rho_s$ , particle size  $d$ , and shear rate  $\dot{\gamma}$  are combined into a single dimensionless ratio of two time scales, microscopic ( $\sqrt{\rho_s d^2 / P_p}$ ) and macroscopic ( $1/\dot{\gamma}$ ):  $I = \dot{\gamma} d / \sqrt{P_p / \rho_s}$  [5–7]. Various articles have shown that dynamic parameters such as the apparent friction coefficient  $\mu = \tau / P_p$  (here,  $\tau$  is a local shear stress) and the solid fraction  $\phi$  can be represented using functions of  $I$  in both steady-state [5] and transient (e.g., column collapse) systems [8]. Cassar *et al.* [9] adapted this framework to submerged particle systems by replacing the microscopic (inertial) timescale with a viscous time scale ( $\eta_f / P_p$ , where  $\eta_f$  is the fluid viscosity), and the appropriate dimensionless control parameter is  $J = \dot{\gamma} \eta_f / P_p$ . Boyer *et al.* [10] further validated the saturated framework and generalized the mathematical form to include much sparser suspensions.

\*manteng@westlake.edu.cn

†khill@umn.edu

‡s.torres@westlake.edu.cn

In the last decade, work on dense flows has broadened to include systems in which both hydrodynamic forces and particle inertial effects contribute to the rheology. Toward this, Trulsson *et al.* [11] proposed an effective shear stress in the form of a linear superposition of inertial and viscous stresses ( $\tau_{\text{eff}} = \lambda \times \rho_s d^2 \dot{\gamma}^2 + \eta_f \dot{\gamma}$  normalized by  $P_p$  that produces a new dimensionless number:  $K = \lambda I^2 + J$ , where  $\lambda$  is a single-valued fitting parameter). Based on their experimental data, Tapia *et al.* [12] argued that  $\lambda = 1/St_{\text{tr}}$ , where  $St_{\text{tr}}$  is a transitional Stokes number ( $St = I^2/J = \rho_s \dot{\gamma} d^2 / \eta_f$ ) close to 1. They observed that  $\phi$  and  $\mu$  exhibit distinct scaling behaviors, thus requiring *two* fitted parameters to collapse their  $\mu$  and  $\phi$  data ( $St_{\text{tr},\mu} = 114$  and  $St_{\text{tr},\phi} = 10$ , respectively).

These efforts have revolutionized the representation of dense suspension flows. However, significant knowledge gaps remain, associated with issues of material properties [12,13] and representations of transitions from inertial-dominated to viscous-dominated dynamics [14]. Recent rheologies based on combinations of  $I$  and  $J$  use single-valued fitted variables to represent the transition from  $I$ - to  $J$ - dominated behaviors [11,12,15], but the lack of physical meaning of these parameters, and the multiple values they can take for the different variable involved ( $\mu$  and  $\phi$ ), greatly limits the physical insight that can be obtained from them.

In this work, we address these points by proposing an alternative *length-scale-based rheology* for dense sheared flows based on the ratio of average relative (“macroscopic”) displacements (associated with streamwise travel in the shearing direction) to deviations from those displacements. The latter (“microscopic” displacements), are increasingly restricted relative to the streamwise displacements as the system  $\phi$  approaches its maximum value  $\phi_c$ . We start by using a conceptualized model to show how near  $\phi_c$  dynamics are partially represented in increasingly limited streamwise-normal movements (compared to streamwise movements) as the system deviates from  $\phi_c$ . Through the momentum balance equation at particle scale, we demonstrate that  $\mu$  depends on three factors: interparticle friction  $\mu_p$ , solid structure (which can be represented by the length-scale ratio), and fluid-structure interaction (which is a function of rescaled confining pressure  $I/J = \sqrt{\rho_s P_p d} / \eta_f$ , which is introduced in the work of Trulsson *et al.* [11]). Then, we theoretically derive the appropriate length-scale ratio between average displacements and average variants from those displacements to model how the ratio varies with solid and fluid properties and forcing conditions. This gives rise to a structure-based rheological parameter that requires *no* fitting parameters and includes a function of the Stokes number  $St_{\text{tr}}$  that varies through the inertial-to-viscous transition, intrinsically capturing the transition for all values of  $\phi/\phi_c$  within the dense flow regime [16]. Moreover, we present a unified expression for  $\mu/\mu_c$  based on a function involving the structural parameter (length-scale ratio), and the fluid-structure interaction parameter  $I/J$ . We demonstrate that the new lengthscale-based framework contextualizes previously proposed time-scale-based frameworks, and also fits published experimental and computational data [10,12,15,17,18].

## II. THEORETICAL DERIVATION OF GENERALIZED LENGTH-SCALE AND TIME-SCALE RATIOS

We begin with a two dimensional (2D) conceptual model of one particle among a conglomeration of particles sheared under uniform shear and normal stresses  $\tau$  and  $P_p$  [Fig. 1(a)] in a fluid with a viscosity of  $\eta_f$ . For a shear rate of  $\dot{\gamma}$ , the average streamwise velocity between particles in layer  $i + 1$  and  $i$  is  $\approx d\dot{\gamma}$ . During the *macroscopic* time scale  $1/\dot{\gamma}$  our particle in the layer  $i + 1$  [ in Fig. 1(b)] moves streamwise by  $\approx d$ . It also moves down and up in the  $y$  – direction, a distance “ $\delta$ ”, e.g., Fig. 1(b)–1(d). In this context we consider how a representative solid fraction varies based on different values of  $\delta$  corresponding to different forcing conditions. We calculate this representation as  $\phi_c = V_p/V_s$ , in which  $V_p$  represents the solid volume contained in triangle ABC ( $\pi d^2/8$  in all cases) and  $V_s$  is the total space. When  $\dot{\gamma}$  is relatively low and  $P_p$  high, a particle in layer  $i + 1$  remains in contact with particles in layer  $i$  and it travels a maximum vertical distance [Fig. 1(c)], generating a dense packing  $\phi_c = V_p/V_{s,\text{min}}$ , where  $V_{s,\text{min}} = \sqrt{3}d^2/4$  is the space required by the three particles in this dense configuration, represented as the equilateral triangle ( $\triangle ABC$ ). In contrast, when  $P_p$  is low and/or  $\dot{\gamma}$  is high, we expect our particle  $A$  to break contact with particle  $B$  in layer  $i$  before

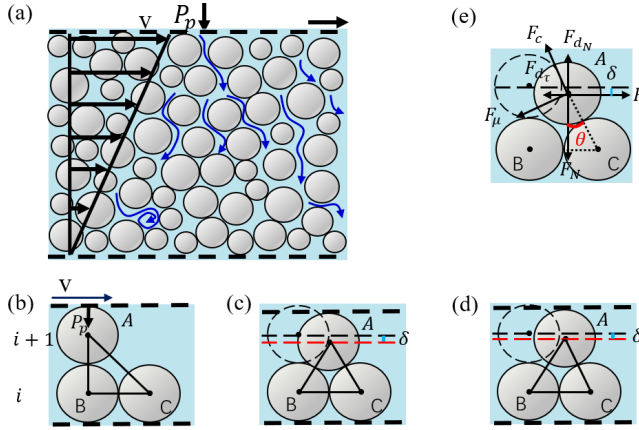


FIG. 1. (a) Shear behavior of dense suspensions: The top plate applies a pressure  $P_p$  on the particles, inducing shear within the granular assembly as the top plates move at a velocity  $v$ , while the bottom plate remains fixed. (b) Schematic of a 2D conceptual model of a particle in layer  $i + 1$  subjected to shear and normal stresses over particles in layer  $i$ . (c) Relative motion for low  $\dot{\gamma}$  (and/or high  $P_p$ ). (d) Relative motion for higher  $\dot{\gamma}$  (and/or lower  $P_p$ ). (e) Force analysis of the particle A during shear.

connecting with  $C$ , reducing the value for  $2\delta$ , e.g., Fig. 1(b)–1(d). Hence, a general expression of the space required by the three particles is  $V_s = d(d - \delta)/2$ , and, a representative solid fraction ratio may be expressed by:

$$\frac{\phi}{\phi_c} = \frac{\sqrt{3}d^2/4}{d(d - \delta)/2} = \frac{\sqrt{3}}{2(1 - \frac{\delta}{d})} = f(d/\delta). \quad (1)$$

This shows that  $\phi/\phi_c$  is dependent on the internal structure identified by  $\delta/d$ . This suggests the importance of displacement length scales in capturing the evolution of the solid fraction.

We continue using the same conceptual model to analyze the likely physical parameters needed for the stress ratio  $\mu = \tau/P_p$  [Fig. 1(e)]. In the quasisteady state, momentum transfer per particle in one layer can be described as follows:  $F_N = \pi d^2 P_p/4$  in the vertical direction and  $F_\tau = \pi d^2 \tau/4$  in the shearing direction. In a densely packed suspension where  $\phi \rightarrow \phi_c$ , there is little space for a particle to fluctuate. The fluid flow inside the dense suspension is a result of fluid-granular interaction, distinct from fluid flow through a porous medium, in which the solid phase is essentially rigid and thus the fluid velocity can be considerably higher than that of the solid phase. In this condition, the relative velocity between the fluid and solid phases is small, resulting in a low Reynolds number. Consequently, we assume that the hydrodynamic force of the particle inside a dense suspension is the Stokes force. We aspire to achieve a comprehensive description of the hydrodynamic forces under various conditions. However, it is a significant challenge that requires a substantial breakthrough in fluid mechanics. While the Stokes force may not encompass all aspects of the dense suspension system's behavior, its use to represent fluid-particle interactions can still enhance our understanding of the interplay between fluid dynamics and inertial effects in this complex system.

To that end, we now express the fluid force (Stokes drag) scaling along with other forces on Particle A at the time interval indicated in Fig. 1(e). Particle A is subjected to Stokes drag in both vertical ( $F_{dN} = 3\pi\eta_f v_N^* d$ ) and shear directions ( $F_{d\tau} = 3\pi\eta_f v_\tau^* d$ ), where  $v_N^*$  and  $v_\tau^*$  denote the magnitude of relative velocities between the fluid and the particle in the vertical and shear directions, respectively. The frictional force between particles A and C scales as  $F_\mu = \mu_p F_c$ , where  $F_c$  is the magnitude of the contact force in the direction normal to the plane of contact and  $\mu_p$  is the particle

friction coefficient. Hence, we can obtain

$$F_N = F_c \cos \theta - \mu_p F_c \sin \theta + 3\pi \eta_f v_N^* d = \pi d^2 P_p / 4, \quad (2a)$$

$$F_\tau = F_c \sin \theta + \mu_p F_c \cos \theta + 3\pi \eta_f v_\tau^* d = \pi d^2 \tau / 4. \quad (2b)$$

The apparent frictional coefficient  $\mu = \tau / P_p$  can be expressed as

$$\mu = \frac{12\eta_f v_\tau^*}{P_p d} + \frac{\left(1 - \frac{12\eta_f v_N^*}{P_p d}\right)(\tan \theta + \mu_p)}{1 - \mu_p \tan \theta}. \quad (3)$$

We define the characteristic velocity  $v_N^*$  as the final velocity of a particle settling in fluid over a distance of a particle diameter  $d$  under  $P_p$ , and  $t_\mu$  is the traveling time. We can obtain  $v_N^* = \frac{P_p d}{12\eta_f} (1 - h(I/J))$ , where  $h(I/J) = e^{-216J^2/I^2 - 1 - W(-e^{-216J^2/I^2 - 1})}$ , where  $W(\cdot)$  is the Lambert-W function. We calculate the shear velocity via  $v_\tau^* = \tan \theta_v v_N^*$ , where  $\theta_v = \theta$  if we approximate the direction of velocity perpendicular to the plane of contact. Refer to Appendices A and B for detailed calculations. We identify a contact angle:

$$\tan \theta = \frac{\sqrt{d^2 - (d - \delta)^2}}{d - \delta} = \sqrt{\left(\frac{1}{1 - \delta/d}\right)^2 - 1}, \quad (4)$$

we can express the apparent frictional coefficient as

$$\mu = (1 - e^{-h(I/J)}) \tan \theta_v + \frac{e^{-h(I/J)}(\tan \theta + \mu_p)}{1 - \mu_p \tan \theta} = g(\mu_p, d/\delta, I/J, \tan \theta_v). \quad (5)$$

To summarize,  $\mu$  depends on three key components, represented by three dimensionless variables: (1) Particle scale friction  $\mu_p$ , which directly impacts momentum exchange between sheared particle layers; (2) The solid skeleton structure represented by the ratio  $d/\delta$  (or  $\phi/\phi_c$ , due to  $d/\delta = f^{-1}(\phi/\phi_c)$ ), as shown in Eqs. (3) and (4). (3) Fluid-structure interaction denoted by  $I/J$  in various systems. Given a specific particle distribution and particle friction, i.e., keeping  $d/\delta$  and  $\mu_p$  constant, variations in fluid and solid properties result in different momentum exchanges. As  $I/J$  increases from 0 to infinity, signifying a decrease in the role of fluid effect from maximum to minimum, Eq. (5) undergoes the following transition:

$$\lim_{I/J \rightarrow 0} \mu = \frac{\tan \theta + \mu_p}{1 - \mu_p \tan \theta}, \quad (6a)$$

$$\lim_{I/J \rightarrow +\infty} \mu = (1 - e^{-1}) \tan \theta_v + \frac{e^{-1}(\tan \theta + \mu_p)}{1 - \mu_p \tan \theta}. \quad (6b)$$

This implies that when fluid-structure interaction reaches its maximum or becomes negligible,  $\mu$  becomes independent of  $I/J$ . This observation aids us in establishing a unifying expression for the rheological model, a discussion of which follows. Although the dynamic process of granular material during shearing is much more complex, this simplified conceptual model still provides physical insights into the behavior of granular materials and allows us to use a length-scale ratio to build a rheological model.

We next derive a quantitative expression for what we might call a ‘‘microscopic’’ length scale  $l_\mu$  in the context of representative forces on a particle. This is analogous to  $\delta$ , as conceptualized above, though the direction of  $l_\mu$  is arbitrary. As previously noted by Cassar *et al.* [9], when inertia, drag force, and  $P_p$  are all significant, we may write:

$$(\pi/6)\rho_s d^3 \frac{dv}{dt} = (\pi/4)P_p d^2 - F_d, \quad (7)$$

for the response of a particle to a contact force on one side (scaling with  $P_p$ ), in a viscous fluid, with no particle contact on the other side (e.g., due to a ‘‘hole’’ in the contact network). As discussed earlier, we assume that a particle within the dense suspension is subjected to a Stokes drag, expressed as  $F_d = 3\pi \eta_f v d$ . We integrate Eq. (7) to find the speed  $v(t)$  and the distance traveled  $l(t)$  for a

particle released from rest:

$$v(t) = \int_{t'=0}^t [dv(t')/dt']dt' = v_f(1 - e^{-t/t_0}), \quad (8a)$$

$$l(t) = \int_{t'=0}^t v(t')dt' = v_ft - v_ft_0(1 - e^{-t/t_0}). \quad (8b)$$

$v_f = P_p d / (12\eta_f)$  is analogous to a settling velocity, and  $t_0 = (\rho_s d^2) / 18\eta_f$ , to a settling time scale. We use Eq. (8b) to derive either a “microscopic time scale”  $t_\mu$  for a particle to travel distance  $l = d$  or a “microscopic length scale”  $l_\mu$  a particle can travel in time  $\mathcal{T} = 1/\dot{\gamma}$ :

$$t_\mu = \frac{12\eta_f}{P_p} + \frac{\rho_s d^2}{18\eta_f} \left[ 1 + W\left(-e^{-216\eta_f^2 / (\rho_s d^2 P_p)}\right) \right], \quad (9a)$$

$$l_\mu = \frac{P_p d}{12\eta_f \dot{\gamma}} - \frac{P_p d^3 \rho_s}{216\eta_f^2} \left( 1 - e^{-18\eta_f / (\rho_s d^2 \dot{\gamma})} \right), \quad (9b)$$

where  $W(\cdot)$  is the Lambert-W function. See Appendix A for calculation details.

With these, we find a dimensionless time- scale ratio by dividing  $t_\mu$  by the (“macroscopic”) timescale  $\mathcal{T} = 1/\dot{\gamma}$ :

$$\Gamma = \frac{t_\mu}{\mathcal{T}} = 12J + \frac{\text{St}}{18} \left[ 1 + W\left(-e^{-216J/\text{St}-1}\right) \right], \quad (10)$$

and a dimensionless length-scale ratio by dividing a (“macroscopic”) length scale  $\mathcal{L} = d$  by  $l_\mu$ :

$$G = \frac{\mathcal{L}}{l_\mu} = \frac{216J^2}{18J - I^2(1 - e^{-18/\text{St}})} = 12(J + \lambda_{\text{St}} I^2); \quad (11a)$$

$$\lambda_{\text{St}} = \frac{(1 - e^{-18/\text{St}})}{18 - \text{St} \times (1 - e^{-18/\text{St}})}. \quad (11b)$$

### III. RELATIONSHIPS AMONG RHEOLOGICAL VARIABLES: $G$ AND $\Gamma$ VS $I, J, K$

The relationship between  $G$  and  $K$  is apparent. The expressions are nearly identical, except for the need for a fitting parameter  $\lambda$ . In the case of  $K$ ,  $\lambda = \lambda_o$ , is a constant that needs to be determined based on the system e.g., material properties and boundary conditions. In the case of  $G$ ,  $\lambda = \lambda(\text{St})$ , a variable that adjusts naturally to the system as it transitions between  $J$  and  $I$  and thus has one fewer fitting parameter.

When the inertial force is dominant over the hydrodynamic force ( $\text{St} \gg 1$ ), we find

$$\lim_{\text{St}/J \rightarrow +\infty} \Gamma = \frac{2I}{\sqrt{3}} \left[ 6\sqrt{3}\sqrt{\frac{J}{\text{St}}} + \frac{\sqrt{3}}{36}\sqrt{\frac{\text{St}}{J}} + \frac{\sqrt{3}}{36}\sqrt{\frac{\text{St}}{J}} W\left(-e^{-\frac{216J}{\text{St}}-1}\right) \right] \quad (12)$$

$$= \frac{2I}{\sqrt{3}} \times \frac{\sqrt{3}}{36} \sqrt{\frac{\text{St}}{J}} [1 + W\left(-e^{-\frac{216J}{\text{St}}-1}\right)]. \quad (13)$$

We use  $\lim_{\text{St}/J \rightarrow +\infty} W\left(-e^{-216J/\text{St}-1}\right) = W(-1/e) = -1$ , and then apply the Taylor expansion to  $W(x)$  as  $x \rightarrow -1/e$ . In that limit  $W(x) = -1 + \sqrt{2(1+ex)} - \mathcal{O}(1+ex)$  [cf. 19]. Thus,

$$\lim_{\text{St}/J \rightarrow +\infty} \Gamma = \frac{2I}{\sqrt{3}} \frac{\sqrt{3}}{36} \sqrt{\frac{\text{St}}{J}} \left[ \sqrt{2(1 - e^{-\frac{216J}{\text{St}}})} - \mathcal{O}(1 - e^{-\frac{216J}{\text{St}}}) \right] \quad (14)$$

$$= \frac{2I}{\sqrt{3}} \frac{\sqrt{3}}{36} \sqrt{\frac{\text{St}}{J}} \left[ \sqrt{\frac{2 \times 216J}{\text{St}}} - \mathcal{O}\left(\frac{216J}{\text{St}}\right) \right] \quad (15)$$

$$= \frac{2I}{\sqrt{3}} \left[ 1 - \mathcal{O}\left(6\sqrt{3}\sqrt{\frac{J}{\text{St}}}\right) \right] \approx 2I/\sqrt{3}. \quad (16)$$

TABLE I. Near  $-\phi_c$  dynamics and rheological parameters for viscous to inertial behaviors ( $St \approx 0 \rightarrow \infty$ )

Flow regimes	Published $\Delta\phi(P_p, \dot{\gamma})$	$\Gamma = t_f/\mathcal{T}$	$G = \mathcal{L}/l$
Viscous ( $St \rightarrow 0$ )	$\frac{\phi_c}{\phi} - 1 \propto J^{0.5}$ [9,10]	$\lim_{St/J \rightarrow 0} \Gamma = 12J$	$\lim_{St \rightarrow 0} G = 12J$
Inertial ( $St \rightarrow \infty$ )	$\frac{\phi_c}{\phi} - 1 \propto I$ [5-7]	$\lim_{St/J \rightarrow \infty} \Gamma = \frac{2}{\sqrt{3}}I$	$\lim_{St \rightarrow \infty} G = \frac{4}{3}I^2$
Visco-inertial ( $St \approx 0 \rightarrow \infty$ )	$\phi_c - \phi \propto \sqrt{K}$ [11,12] <sup>a</sup> $\frac{\phi_c}{\phi} - 1 \propto \sqrt{K}$ [15]	$\frac{\phi_c}{\phi} - 1 \propto \Gamma^\alpha$ $\alpha = 0.5 \rightarrow 1^b$	$\frac{\phi_c}{\phi} - 1 \propto G^{0.5}$

<sup>a</sup> $K = \lambda_i J^2 + J$ ; where  $\lambda_i$  is a fit parameter that can have two values, one each for  $i = \phi$  or  $\mu$  [12];

<sup>b</sup> $\Gamma$  and  $G$  are in Eqs. (10) and (11).  $\alpha$  is a fit parameter for  $\Gamma$ . No fit parameters are needed for  $G$ .

For the dimensionless length scale

$$\lim_{St \rightarrow +\infty} G = \frac{216J^2}{18J - I^2(1 - e^{-18J/I^2})} = \frac{216J}{18 - St(1 - e^{-18/St})} \quad (17)$$

$$= \frac{216J}{18 - St\left(\frac{18}{St} - \frac{9 \times 18}{St^2} + \frac{3 \times 18^2}{St^3} - \mathcal{O}\left(\frac{1}{St^4}\right)\right)} = \frac{216J}{\frac{9 \times 18}{St} - \frac{3 \times 18^2}{St^2} - \mathcal{O}\left(\frac{1}{St^3}\right)} \quad (18)$$

$$= \frac{4J \times St}{3 - \frac{18}{St} - \mathcal{O}\left(\frac{1}{St^2}\right)} \approx 4I^2/3. \quad (19)$$

In other words, in the limit of large  $St$ ,  $\Gamma$  recover to the inertial number (time ratio in inertial regime), while,  $G$  transform into a square of the inertial number. Albeit subtle, this difference in the exponent of  $I$  is critical as will be shown later on. When the hydrodynamic force is dominant, one obtains

$$\lim_{St/J \rightarrow 0} \Gamma = 12J\left[1 + \frac{St}{216J} + \frac{St}{216J}W\left(-e^{-\frac{216J}{St}-1}\right)\right] = 12J, \quad (20)$$

where  $W(0) = 0$ . The dimensionless length scale is

$$\lim_{St \rightarrow 0} G = \frac{216J^2}{18 - St(1 - e^{-18/St})} \approx \frac{216J^2}{18J} = 12J. \quad (21)$$

In the limit of small  $St$ , both  $\Gamma$  and  $G$  have the same limiting value:  $\approx 12J$ . As granular materials change from a free fall regime to a viscous regime, the generalized time-scale ratio  $\Gamma$  naturally transforms from the inertial number  $I$  (time-scale ratio in inertial regime defined in work of [5]) to the viscous number  $J$  (time-scale ratio in inertial regime defined in the work of Ref. [9]), when ignoring the constant parameter. However,  $G$  naturally recovers the transition from the inertial number based  $(\phi_c/\phi - 1) \propto I \propto \sqrt{G}$  in the inertial regime to the viscous number based  $(\phi_c/\phi - 1) \propto J^{0.5} \propto \sqrt{G}$  in the viscous regime. This is another argument supporting the choice of  $G$  as the key dimensionless parameter.

We summarize some details in Table I including their relationships with  $I$ ,  $J$ , and  $K$ . The first column details conditions for comparisons (i.e., high, low, and moderate  $St$ ). The second column summarizes previously published relationships for  $I$ ,  $J$ , and  $K$ . In the third and fourth columns, we see that in the high- $St$  limits,  $\Gamma$  and  $\sqrt{G}$  scale identically with  $I$ . However, at the lowest values of  $St$ ,  $\Gamma$  scales with  $J$ , while  $\sqrt{G}$  scales with  $\sqrt{J}$  suggesting the need for an additional fit parameter may be needed for  $\Gamma$  to fully reconcile with the data. In fact, the form of  $G$  is similar to  $K$  with an important difference which will be highlighted later on.

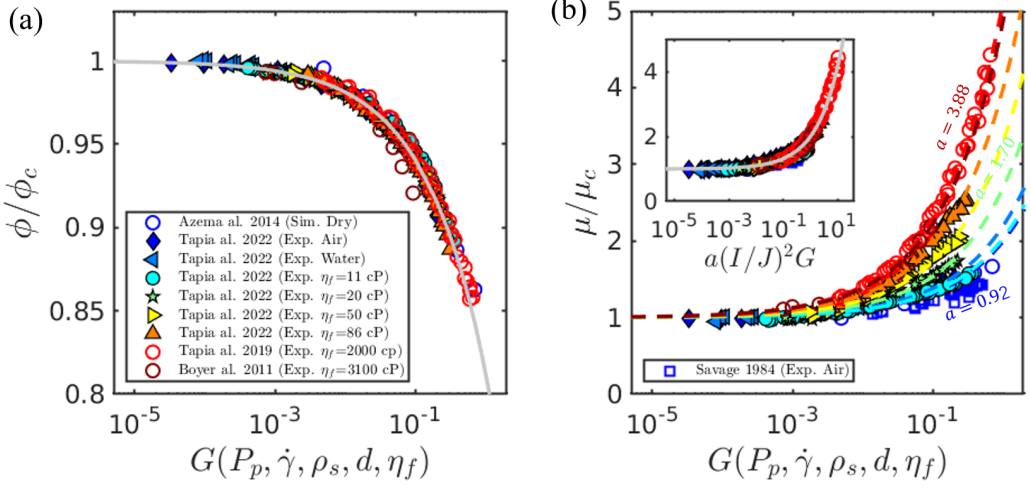


FIG. 2. Normalized solid fraction (a) and apparent frictional coefficient (b) plotted vs. data from  $G$  for data from Refs. [10,12,17,18,20]. The solid line in (a) are from Eq. (22b), using  $b = 0.188$ , and the solid line inset of (b) are from Eqs. (22a) and (23) with  $a_i = 1.0$ ,  $a_u = 4.0$ , and  $c = 41$ .

#### IV. RESULTS

Based on the theoretical analysis in Sec. III, we plot  $\phi/\phi_c$  and  $\mu/\mu_s$  vs  $G$  using previously published experimental and computational data [10,12,17,18,20] in Figs. 2(a) and 2(b). And the rheological parameters can be expressed by previously proposed relationships [12]:

$$\mu = \mu_c(1 + aG^{0.5}), \quad \text{and} \quad (22a)$$

$$\phi = \phi_c(1 - bG^{0.5}). \quad (22b)$$

We determined that  $b \approx 0.188$  remains a constant across all systems, as illustrated in Fig. 3(a), aligning with our analytical findings from the conceptual model.  $\phi/\phi_c = \Phi(G)$  is consistently

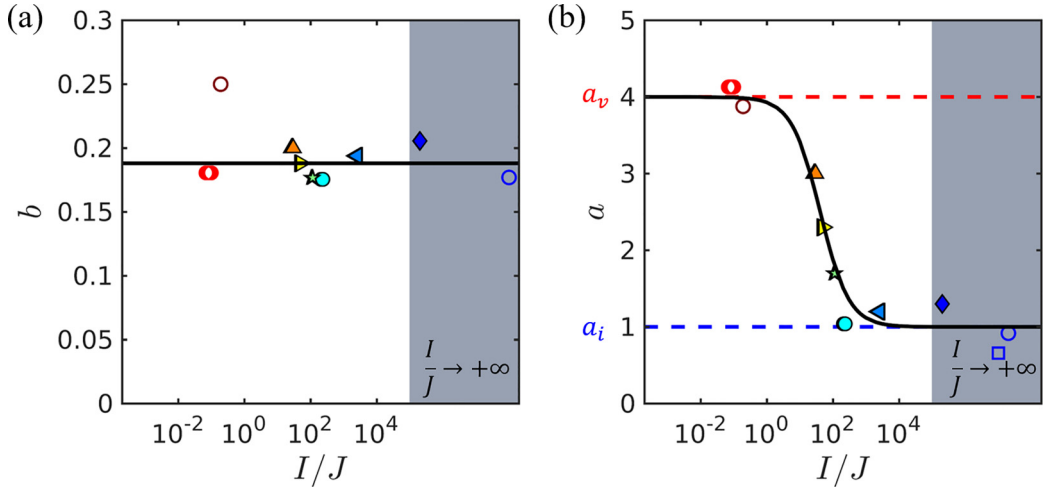


FIG. 3. Evolution of fitting parameter (a)  $b$  and (b)  $a$  vs  $I/J$  for data from Refs. [10,12,17,18]. The solid black line in (b) is from Eq. (23) with  $a_i = 1$ ,  $a_v = 4$ , and  $c = 41$ .

TABLE II. Critical apparent friction and solid fraction.

	$\eta_f$ (cp)	$\phi_c$	b	$\mu_c$	a
Savage [17]	Air	-	-	0.414	0.66
Azéma and Radjaï [18]	Dry	0.578	0.178	0.382	0.92
Tapia <i>et al.</i> [12]	0.0183 (Air)	0.596	0.206	0.394	1.30
Tapia <i>et al.</i> [12]	1	0.586	0.194	0.411	1.20
Tapia <i>et al.</i> [12]	11	0.615	0.176	0.315	1.04
Tapia <i>et al.</i> [12]	20	0.617	0.177	0.315	1.70
Tapia <i>et al.</i> [12]	50	0.615	0.188	0.312	2.30
Tapia <i>et al.</i> [12]	86	0.615	0.200	0.311	3.02
Tapia <i>et al.</i> [20]	2000	0.584	0.181	0.372	4.13
Boyer <i>et al.</i> [10]	3000	0.584	0.250	0.30	3.88

represented by a single function of a structure-based parameter, the length-scale ratio  $G$ . However,  $\mu_c$ ,  $\phi_c$ ,  $a$  are system-dependent parameters. Both  $\phi_c$  and  $\mu_c$  represent critical values in the jamming transitions, and recent work has shown that  $\mu_c$  accounts for the effect of the particle-scale friction  $\mu_p$  [21]. Parameter  $a$  varies, starting from a constant value in dry conditions ( $a_i \approx 1.0$ ) and increasing to a larger constant value in highly viscous conditions ( $a_v \approx 4.0$ ), as depicted in Fig. 2(b). The fitting parameter  $\phi_c$ ,  $\mu_c$ ,  $a$ , and  $b$  for different systems are presented in Table II (refer to Appendix C for details).

As discussed in Sec. II, the introduction of the rescaled confining pressure  $I/J$  is necessary to account for the effect of fluid-solid interaction on  $\mu$ . Consequently, we plot the last fitting parameter  $a$  in Eq. (22a) against  $I/J$  and fit their relationship with

$$a = a_v - \frac{a_v - a_i}{1 + c/(I/J)}, \quad (23)$$

where  $a_v \approx 4.0$  is a constant upper limit at extreme viscous regime [derived from the data of 10,20],  $a_i \approx 1.0$  is a lower limit value in the dry condition [derived from the data of 12,17,18]. The parameter  $c = 41$  is a fitted constant parameter. Equation (23) demonstrates that for a fixed  $G$  (in relation to a specific  $\phi/\phi_c$ , assuming the similar internal solid structure) within a P-imposed system with constant particle friction  $\mu_p$ , increasing the fluid viscosity from 0 to a high value (resulting in a decrease of  $I/J$  from infinity to 0) leads to a progression in the influence of the fluid, transitioning from negligible to a peak. This aligns with the theoretical analysis presented in our conceptual model.

As depicted in Fig. 4(a), we observe scaling relations between  $\phi/\phi_c$  and the general form of the time scale ratio  $\Gamma^\alpha$  as the system transform from an inertial to viscous regime, the exponent  $\alpha$  undergoes a transition from 1.0 to 0.5. We find  $\Gamma$  impractical and do not consider it further herein. In contrast,  $G$  does not require such a compromise. This study confirms recent discoveries showcasing distinct scaling laws for  $\phi$  and  $\mu$  [cf. 12]. We attribute this discrepancy to the variations in fluid-structure interaction as a function of  $I/J$ , as elucidated through theoretical analysis using our conceptual model [see Eq. (5)]. Furthermore, we propose a universal constitutive law among different systems. The root mean square error for predicting  $\mu$  using the data from [12] decreases from  $2.2e-3$  to  $4.3e-4$  when utilizing Eq. (22a) in comparison to their established relations.

Before we conclude, we briefly revisit the question of appropriate system scales. As we recall,  $I$  and  $J$  were derived using ratios of macro- to micro- time scales for inertial and viscous systems, respectively, while the intentionally-designed cross-rheology parameter  $K$  was initially proposed based on a linear superposition of stress scales [11] (similar to  $I_m = \sqrt{\alpha_1 I^2 + \alpha_2 J}$  [cf. 15]). Starting

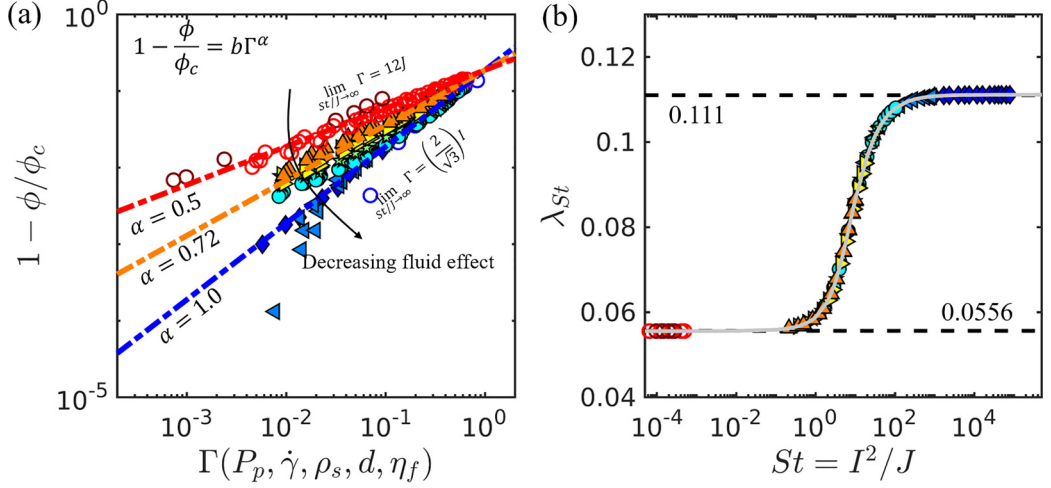


FIG. 4. (a)  $1 - \phi/\phi_c$  vs generalized time-scale ratio  $\Gamma$ , where  $\Gamma$  transforms from an inertial number  $(2/\sqrt{3})I$  to a viscous number  $12J$  and  $\alpha = 0.5 \rightarrow 1$  as the fluid-granular system varies from a dry condition to a very viscous condition, the dash line is plotted by  $1 - \phi/\phi_c = 0.188\Gamma^\alpha$  with  $\alpha = 0.5, 0.72,$  and  $1$ . (b) shows  $\lambda$  vs  $St$ , the solid line is plotted by Eq. (11b).

from these superpositions ends with forms that require additional fit parameters ( $\lambda_o$  or  $\lambda_\mu$  and  $\lambda_\phi$  for  $K$  or  $\alpha_1/\alpha_2$  for  $I_m$ ). Our new time-scale ratio  $\Gamma$  provides a generalized form of  $J$  and  $I$  from the viscous regime to the inertial regime. However, it still requires a fit parameter  $\alpha$ , that varies from  $1/2$  to  $1$  as the system transitions from viscous to inertial (Table I). While undesirable, this is still intuitive: it forces a transition between a  $\dot{\gamma}$ -rheology in the viscous limit to a  $\dot{\gamma}^2$ -rheology in the inertial limit, as shown previously to hold for these systems [10,12]. Our new length-scale ratio  $G$  does not require a fitting parameter and, at the same time, contains the functional form of  $\lambda(St)$  necessary to transform  $G$  into  $K$  Eq. (11b). The length-scale can effectively capture the evolution of  $\phi/\phi_c$  of the granular assembly. Furthermore, the length-scale ratio combined with  $I/J$  can better capture the evolution of  $\mu/\mu_c$ . The importance of length scales is highlighted by the proposed conceptual model. We elaborate on additional relationships between the length-scale ratio and macroscopic properties  $\phi$  and  $\mu$  through this conceptual model along with force analysis and geometric operation. The proposed constitutive relations Eqs. (22a), (22b), and (23)] provide a precise reflection and correlation with the physical influencing factors for each rheological parameter. For example,  $\phi/\phi_c = f(d/\delta) = \Phi(G)$ , and  $\mu = g(\mu_p, d/\delta, I/J) = \mathcal{G}(\mu_c, G, I/J)$ , where  $G$  is analogous to  $d/\delta$  and  $\mu_c$  represents the effect of  $\mu_p$  [21].

In addition to the rheological studies reviewed here, studies of near-jammed (near  $\phi_c$ ) systems have illustrated that spatial structures play important roles during particle transport [e.g., 16,22,23]. For example, the dynamical processes of granular flows are strongly correlated to larger-scale correlated movements within a granular assembly. While the relationships between the structures and flows remain open questions, we have provided significant justifications to give renewed importance to the proposed length-scale ratios over the existing alternatives.

## V. CONCLUSIONS

To summarize, in this work, we considered the inertial response of a sphere subjected to contact pressure  $P_p$  and a linear drag force, and derived a particle-response micro-time scale  $t_\mu = t(l = d)$  and equivalent micro-length scale  $l_\mu = l(t = 1/\dot{\gamma})$ , i.e., the time for a particle to travel by  $d$  and the distance for a particle to travel in time  $1/\dot{\gamma}$ , respectively, in response to this forcing. From these, we derived a time-scale ratio and a length-scale ratio:  $\Gamma = t_\mu/(1/\dot{\gamma})$  and  $G = d/l_\mu$ . When considering

these in the context of previously published data, we found that the length-scale ratio (rather than a time-scale ratio) is intrinsically related to the  $\phi/\phi_c$  and requires no additional fitting parameters in comparison with existing alternatives. The apparent frictional coefficient  $\mu$  is influenced by three key components: particle-particle friction  $\mu_p$ , solid structure, and the fluid-structure interaction. Previous research [21] has shown that  $\mu_c$  is influenced by  $\mu_p$ , and our study demonstrates that the solid structure is accurately characterized by the proposed  $G$ . Additionally, the effect of the fluid-structure interaction is universally captured by a function of  $I/J$ .

Based on these results along with recent work connecting particle properties with rheology parameters [21], we propose general constitutive relationships suitable for a wide range of dense, sheared granular flows across the viscous-inertial transition expressed using dimensionless scales  $G$  and  $I/J$  where the effects of viscous drag and inertia change under different confining pressures, fluid viscosities, and macroscopic deformations. These results provide insight toward expanding our understanding of the influence of different lengthscales in dense particle-fluid flows, providing a greater promise for formulating constitutive models for larger-scale physics-based flow than the ones we explored herein.

In our current study, the derivation of the length-scale ratio relies on the assumption of Stokes' law. However, in cases where Stokes' law may not be applicable, a more precise expression for hydrodynamic effects or an additional force field is necessary to derive the length scale accurately. Nevertheless, we have presented a physically grounded conceptual model that can be extended to comprehend the dynamics of complex dense granular systems.

#### ACKNOWLEDGMENTS

This work is supported by the National Natural Science Foundation of China (NSFC Grants No. 12172305 and No. 12202367) and the U.S. National Science Foundation under Grants No. EAR-2127476 and No. EAR-1451957.

#### APPENDIX A: DERIVATION DETAILS FOR MICROSCOPIC TIME $t_\mu$

As defined by Cassar *et al.* [9], the microscopic characteristic time scale  $t_\mu$  is the time it takes for a particle to travel for a distance of  $d$ . From Eq. (8b),

$$d = v_f t_\mu - v_f t_0 (1 - e^{-t_\mu/t_0}), \quad (\text{A1})$$

where  $v_f = P_p d / (12\eta_f)$ ,  $t_0 = (\rho_s d^2) / 18\eta_f$ . With some algebra we can obtain

$$\frac{1}{t_0} \left( t_\mu - t_0 - \frac{d}{v_f} \right) \exp \left[ \frac{1}{t_0} \left( t_\mu - t_0 - \frac{d}{v_f} \right) \right] = -\exp \left[ - \left( 1 - \frac{d}{t_0 v_f} \right) \right]. \quad (\text{A2})$$

Equation (A2) has the form of the Lambert W-function, and  $X$  can be calculated using the Lambert W-function  $W$  as  $X = W(Y)$  [24]. Hence, the solution for  $t_\mu$  is expressed as

$$t_\mu = \frac{d}{v_f} + t_0 + t_0 W \left( - e^{-d/(t_0 v_f) - 1} \right) \quad (\text{A3})$$

$$= \frac{12\eta_f}{P_p} + \frac{\rho_s d^2}{18\eta_f} \left[ 1 + W \left( - e^{-216\eta_f^2 / (\rho_s d^2 P_p) - 1} \right) \right] \quad (\text{A4})$$

$$= \frac{12\eta_f}{P_p} + \frac{\rho_s d^2}{18\eta_f} \left[ 1 + W \left( - e^{-216J^2 / I^2 - 1} \right) \right]. \quad (\text{A5})$$

**APPENDIX B: DERIVATION DETAILS FOR CHARACTERISTIC VELOCITY  $v_n^*$** 

We can calculate the characteristic velocity  $v_N^* = v_\tau^* / \tan \theta_v = v(t_\mu)$  in vertical direction with Eq. (8a),

$$v_N^* = \frac{P_p d}{12\eta_f} \left( 1 - e^{-t_\mu \frac{18\eta_f}{\rho_s d^2}} \right) = \frac{P_p d}{12\eta_f} \left[ 1 - e^{-216\eta_f^2 / (\rho_s P_p d^2) - 1 - W(-e^{-216J^2 / I^2 - 1})} \right] \quad (\text{B1})$$

$$= \frac{P_p d}{12\eta_f} \left[ 1 - e^{-216J^2 / I^2 - 1 - W(-e^{-216J^2 / I^2 - 1})} \right] \quad (\text{B2})$$

$$= \frac{P_p d}{12\eta_f} [1 - h(I/J)], \quad (\text{B3})$$

where

$$h(I/J) = e^{-216J^2 / I^2 - 1 - W(-e^{-216J^2 / I^2 - 1})}. \quad (\text{B4})$$

Hence, Eq. (5) is given by

$$\mu = \frac{12\eta_f v_\tau^*}{P_p d} + \frac{\left(1 - \frac{12\eta_f v_N^*}{P_p d}\right) (\tan \theta + \mu_p)}{1 - \mu_p \tan \theta} \quad (\text{B5})$$

$$= \tan \theta_v [1 - h(I/J)] + \frac{h(I/J) (\tan \theta + \mu_p)}{1 - \mu_p \tan \theta}. \quad (\text{B6})$$

Due to  $\tan \theta$  is a function of  $d/\delta$ ,

$$\mu = g(\mu_p, d/\delta, I/J, \tan \theta_v). \quad (\text{B7})$$

**APPENDIX C: CRITICAL VALUES**

The critical solid fraction, apparent friction, and the best fit parameter  $a$  and  $b$  in Eqs. (22a) and (22b) in different works are listed in Table II.

- 
- [1] K. Hutter, T. Koch, C. Pluüss, and S. B. Savage, The dynamics of avalanches of granular materials from initiation to runout. Part II. experiments, *Acta Mech.* **109**, 127 (1995).
  - [2] P. Tegzes, T. Vicsek, and P. Schiffer, Avalanche dynamics in wet granular materials, *Phys. Rev. Lett.* **89**, 094301 (2002).
  - [3] G. C. Yang, L. Jing, C. Y. Kwok, and Y. D. Sobral, Pore-scale simulation of immersed granular collapse: Implications to submarine landslides, *J. Geophys. Res.* **125**, e2019JF005044 (2020).
  - [4] K. Kamrin, Non-locality in granular flow: Phenomenology and modeling approaches, *Front. Phys.* **7**, 116 (2019).
  - [5] G. MiDi, On dense granular flows, *Eur. Phys. J. E* **14**, 341 (2004).
  - [6] F. da Cruz, S. Emam, M. Prochnow, J.-N. Roux, and F. Chevoir, Rheophysics of dense granular materials: Discrete simulation of plane shear flows, *Phys. Rev. E* **72**, 021309 (2005).
  - [7] P. Jop, Y. Forterre, and O. Pouliquen, A constitutive law for dense granular flows, *Nature (London)* **441**, 727 (2006).
  - [8] L. Lacaze and R. R. Kerswell, Axisymmetric granular collapse: a transient 3D flow test of viscoplasticity, *Phys. Rev. Lett.* **102**, 108305 (2009).
  - [9] C. Cassar, M. Nicolas, and O. Pouliquen, Submarine granular flows down inclined planes, *Phys. Fluids* **17**, 103301 (2005).
  - [10] F. Boyer, É. Guazzelli, and O. Pouliquen, Unifying suspension and granular rheology, *Phys. Rev. Lett.* **107**, 188301 (2011).

- [11] M. Trulsson, B. Andreotti, and P. Claudin, Transition from the viscous to inertial regime in dense suspensions, *Phys. Rev. Lett.* **109**, 118305 (2012).
- [12] F. Tapia, M. Ichihara, O. Pouliquen, and E. Guazzelli, Viscous to inertial transition in dense granular suspension, *Phys. Rev. Lett.* **129**, 078001 (2022).
- [13] T. Man, Q. Feng, and K. Hill, Rheology of thickly-coated granular-fluid systems, [arXiv:1812.07083](https://arxiv.org/abs/1812.07083).
- [14] R. A. Bagnold, Experiments on a gravity-free dispersion of large solid spheres in a Newtonian fluid under shear, *Proc. R. Soc. London A* **225**, 49 (1954).
- [15] L. Amarsid, J.-Y. Delenne, P. Mutabaruka, Y. Monerie, F. Perales, and F. Radjai, Viscoinertial regime of immersed granular flows, *Phys. Rev. E* **96**, 012901 (2017).
- [16] L. Bocquet, A. Colin, and A. Ajdari, Kinetic theory of plastic flow in soft glassy materials, *Phys. Rev. Lett.* **103**, 036001 (2009).
- [17] S. B. Savage, The mechanics of rapid granular flows, *Adv. Appl. Mech.* **24**, 289 (1984).
- [18] E. Azéma and F. Radjai, Internal structure of inertial granular flows, *Phys. Rev. Lett.* **112**, 078001 (2014).
- [19] D. Veberič, Lambert w function for applications in physics, *Comput. Phys. Commun.* **183**, 2622 (2012).
- [20] F. Tapia, O. Pouliquen, and É. Guazzelli, Influence of surface roughness on the rheology of immersed and dry frictional spheres, *Phys. Rev. Fluids* **4**, 104302 (2019).
- [21] T. Man, P. Zhang, Z. Ge, S. A. Galindo-Torres, and K. M. Hill, Friction-dependent rheology of dry granular systems, *Acta Mechanica Sinica* **39**, 722191 (2023).
- [22] J. Choi, A. Kudrolli, R. R. Rosales, and M. Z. Bazant, Diffusion and mixing in gravity-driven dense granular flows, *Phys. Rev. Lett.* **92**, 174301 (2004).
- [23] C. Bonnoit, J. Lanuza, A. Lindner, and E. Clement, Mesoscopic length scale controls the rheology of dense suspensions, *Phys. Rev. Lett.* **105**, 108302 (2010).
- [24] T. C. Scott, R. Mann, and R. E. Martinez Ii, General relativity and quantum mechanics: towards a generalization of the Lambert W function, *Appl. Algebra Eng. Commun. Comput.* **17**, 41 (2006).